Low temperature synthesis and characterization of nanocrystalline TiO_2 thin films

Dadaso B. Shinde[1], Yogesh A. Pawar[1], Yogesh A. Choudhary[1], Ajay P. Nikum[1], Popatrao N. Bhosale[2], Raghunath K. Mane[3].

[1]SPK Mahavidyalaya, Sawantwadi, Sindhudurg, India,

[2]Materials Research Laboratory, Department of Chemistry, Shivaji University, Kolhapur, (MS).

[3]Smt.K.R.P. Kanya Mahavidyalaya, Islampur-415 409, Tal.Walwa, Dist. Sangli, (MS).

Abstract: In the present investigation, we report low temperature facile synthesis of TiO_2 nanocrystalline thin films. TiO_2 nanorods were hydrothermally deposited on transparent conducting oxide substrate comparatively at low temperature (140 ^{0}C). The structural, optical, morphological and compositional properties are investigated by detailed XRD, UV-Vis-NIR spectrophotometer, SEM, EDS and XPS studies. Optical spectra showed strong light absorption in UV region. The XRD, EDS and XPS spectrum demonstrated that the deposited thin films consist pure rutile phase tetragonal TiO_2 nanorods. The SEM images confirm uniform, compact and well aligned nanorods were grown on the overall substrate surface. The deposited nanocrystalline TiO_2 material have potential for solar cell application.

IndexTerms **-** Single crystalline, rutile phase, nanorods.

1. INTRODUCTION

Searching of alternative energy source is a vital issue in the modern civilization for many reasons which include depletion of conventional energy sources like coal, oil, natural gas etc. and burning of these energy fuels leading to a global air pollution problem. Hence there has been increasing interest during the last few decades to find out an alternative cost effective renewable energy sources to fulfill the future energy needs of mankind. In this respect synthesis of tailored morphological transitional metal oxide (TMO) semiconducting thin films because of their widespread applications in optoelectronic fields of science and technology leading to drastic cut in the production cost of semiconducting devices. Exploring novel approaches to produce low cost, high efficiency photovoltaic cells has attracted attention of researchers because of the urgent need for the clean and renewable energy sources [1-2].

TiO_2 is a wide band gap (3.2eV) transition metal oxide semiconductor and it has received increasing attention due to its many unique properties. Various kinds of nanostructured TiO_2 such as nanoparticle, nanorods, nanotubes, hollow sphere, mesoporous and macroporous TiO_2 have been synthesized and used as a photoanode for the PEC application. [3-4].

On the basis of above consideration, we have intent to develop a simple synthetic strategy to fabricate TiO_2 nanorod microstructure for the PEC cell performance. In this work, we have demonstrated relatively lower temperature hydrothermal evolution of TiO_2 nanorod structure with keeping reaction time constant. Such TiO_2 nanorods provide a large surface area and higher absorption of incident photons, which leads to more photogenerated electron–hole pair, causes higher PEC performance [5-6].

2. MATERIALS

Titanium tetraisopropoxide (TTIP)(99.98% Spectrochem, India), Concentrated hydrochloric acid (35.4% Thomas Baker) used as the Ti precursor.

3. THIN FILM SYNTHESIS

In a typical TiO_2 thin film synthesis 0.5 ml titanium tetra isopropoxide (TTIP) was added in aqueous solution containing 1:1 HCl and stirred vigerously to obtained clear and transparent solution. The resultant solution was added into teflon lined stainless steel autoclave. The conducting FTO glass substrate is immersed into autoclave and autoclave was sealed and placed in an oven at 140°C for 5 hr followed by natural cooling to room temperature. The substrate was removed from autoclave, cooled at room temperature and rinsed thoroughly using double distilled water.

4.1. OPTICAL STUDY

UV-Visible absorption spectrum of the deposited TiO_2 thin film in the range of 300-1200 nm is shown in fig.1. Fundamental of absorption corresponds to electron excitation from the valence band to the conduction band using ultraviolet and visible radiation. The absorption spectrum revels the strong absorption from at 370 nm indicated a charge transfer process from the valence band to conduction band in the UV region.

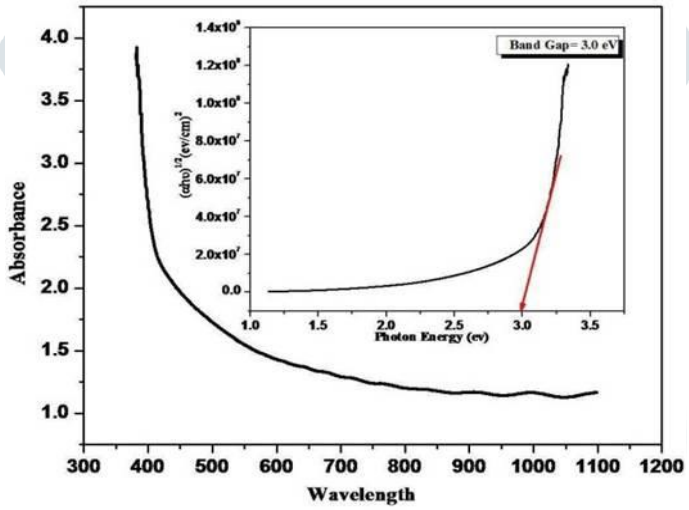

Fig.1 Plot of Absorbance Vs wavelength and inset shows plot of $(\alpha h\upsilon)^2$ Vs. hυ.

Using the absorption edge value, the band gap was calculated using the Tauc relation,

$$\alpha = \frac{A(h\nu - Eg)^n}{h\nu}$$

Where, A is an energy dependent constant, Eg is the band gap energy and hυ is photon energy. The plot of $(\alpha h\upsilon)^2$ Vs. hυ yielded straight line at higher energies indicating direct type of transition. The intercept of the extrapolation to zero absorption with the photon energy axis are taken as the value of band gap Eg. The band gap of deposited TiO_2 thin film was found to be 3.00 eV [7].

4.2. STRUCTURAL STUDY

The crystallite size and crystal structure of TiO_2 thin films was confirmed from the XRD analysis. Fig. 2 shows XRD pattern of TiO_2 thin film. XRD patterns exhibited strong diffraction peaks at 27.55°, 36.79°and 55.40° indicating formation of rutile phase of TiO_2 material. The intense peak at 27.55^0 is the representative peak for (110) plane of rutile TiO_2. All other peaks observed at 36.79^0, 39.12^0, 41.42^0, 44.29^0, 55.40^0, 62.72^0 and 64.29^0, represents (101), (200), (111), (210), (220), (002) and (310) planes respectively which confirms the tetragonal crystal structure of TiO_2 [8-9].

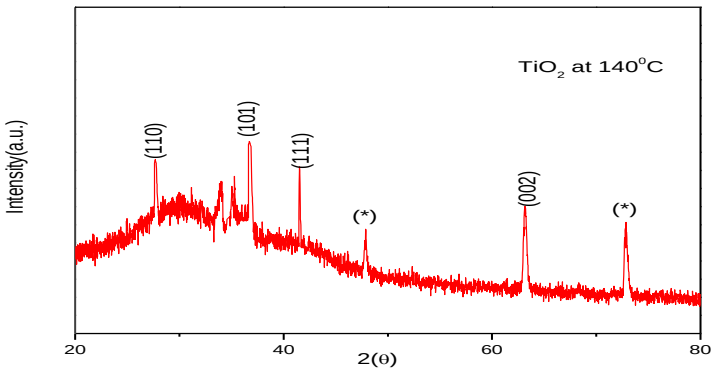

Fig. 2 XRD pattern of TiO_2 thin film sample.

The sample is well crystalline in rutile TiO_2 single crystals, where the growth direction is along (001) orientation and the side surfaces exhibit (110) facets. All peaks are in good agreement with the standard JCPDS data (Card No. 00 001-0562) [10]. The other peaks shown by asterisks are due to the FTO substrate marked by (*).

The presence of broad XRD peak is an indication of small crystallite size in the range of nanoscale, affirming the nanocrystalline nature of the TiO_2 samples [11].

Average crystallite size of TiO_2 samples were 60 nm calculated by using Scherrer's formula,

$$D = \frac{0.94\,\lambda}{\beta \cos\theta}$$

4.3. MORPHOLOGICAL STUDY

The SEM image of the deposited TiO_2 thin film is shown in fig.3 a and b. SEM image clearly shows that the TiO_2 nanorods were deposited on the substrate surface. The uniformly arranged TiO_2 nanorods can provide the faster conduction pathway (less grain boundaries, which associate with traps and barriers) for charge transport [12], and the electron transfer time from the point of carrier generation to the collection electrode is significantly reduced. Hence these micrographs of TiO_2 material are strongly applicable for solar cells application.

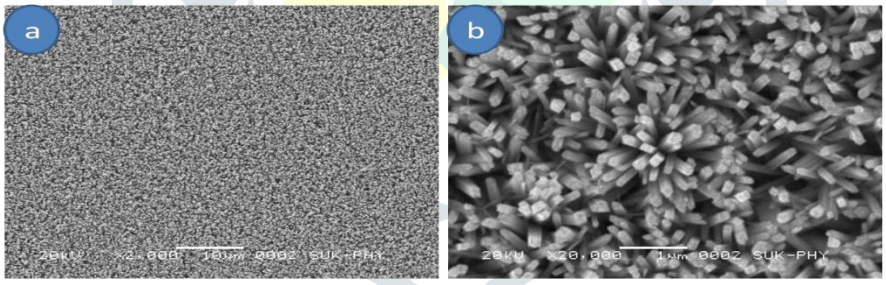

Fig.3 SEM images of TiO_2 thin film smple

4.4. COMPOSITIONAL ANALYSIS

An elemental composition of TiO_2 thin film was analyzed by EDS spectrum. Fig. 4 shows the EDS pattern of TiO_2 thin film sample. There is no trace of any other impurities could be seen within the detection limit of the EDS as presented in Figure. Hence EDS analysis confirms the formation of pure TiO_2 thin film material [13].

The XPS analysis of TiO_2 thin films was performed to identify the composition and valence state of deposited elements. The survey spectrum of sample is presented in Fig. 5(a) which showed presence of Ti, O and a small amount of adventitious carbon. The carbon peak is attributed to the residual carbon from XPS instrument itself [14].

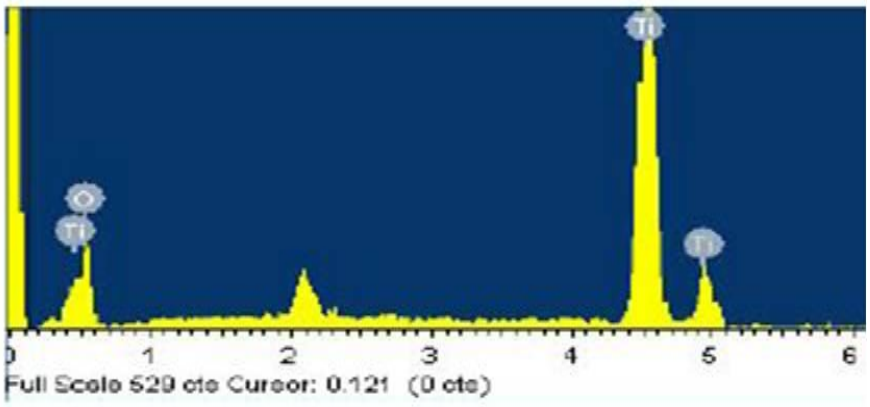

Fig. 4 EDS spectrum of TiO_2 thin film sample.

The peak at binding energy 284.87 eV corresponds to amorphous carbon. Ti 2p spectrum is shown in Fig. 5(b) consists of the distinct Ti $2P_{1/2}$ and Ti $2P_{3/2}$ signals that are located at 464.4 and 458.6 eV respectively. The spin orbital splitting between these peaks is 5.8 eV which is comparable with that of 5.74 eV reported values, indicates Ti^{4+} oxidation state of titanium in TiO_2 [15]. Both Ti 2p signals are highly symmetric, and no shoulders were observed on the lower energy sides of Ti 2p3/2 signal, which indicate that the rutile TiO_2 nanocrystals are stoichiometric and the concentration of lattice defects is extremely low. The core level spectrum of oxygen is shown in Fig. 5(c). It shows a peak at binding energy 529.98 eV. The peak located at 529.98 eV attributed to oxygen originating from lattice oxygen suggesting the presence of surface hydroxyl groups. Thus XPS spectrum confirms the Ti^{4+} and O^{2-} species in TiO_2 thin film [16-18].

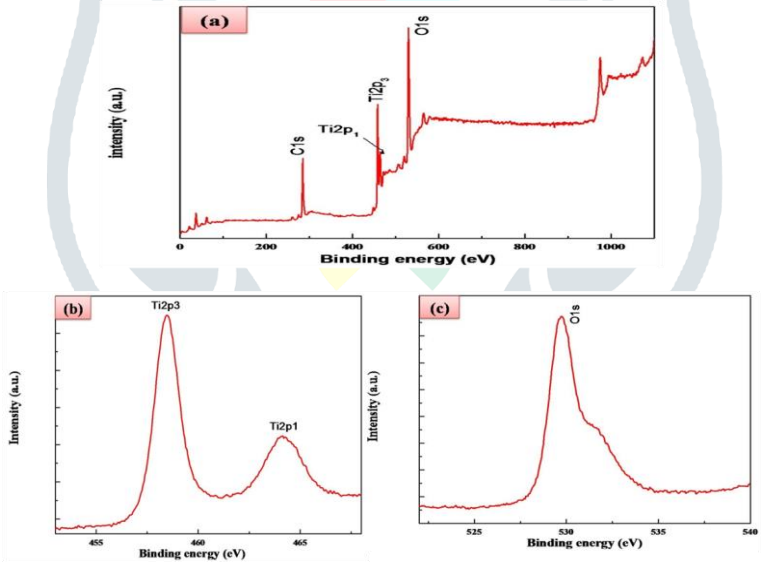

Fig. 5 (a) Survey spectrum of TiO_2,(b) core level spectrum of Ti2P and; (c) core level spectrum of O1s of TiO_2 thin film.

CONCLUSIONS

We have successfully demonstrated synthesis of TiO_2 thin films having well aligned nanorod morphology at relatively lower temperature i.e. 140°C. The deposited thin films consist pure rutile phase tetragonal TiO_2 nanorods, grown uniformly on the overall substrate surface. The structural optical and morphological study showed that the deposited nanocrystalline TiO_2 material have potential for solar cell application.

REFERENCES

1. P. K. Santra and P. V. Kamat, (2012), J. Am. Chem. Soc., 134, (5) 2508-2511.
2. R. Bel-Hadj-Tahar, A. B. Mohamed, (2014), N. J. Glass and Ceramics, (4), 55-65.
3. R. A. Naphade, M. Tathavadekar, J. P. Jog, S. Agarkar and S. Ogale, (2014), J. Mater. Chem. A, (2), 975-984.
4. E. Guo and L. Yin, (2015), J. Phys. Chem., 17, 563-574.
5. A. I. Ali, A. H. Ammar, A. A. Moez, (2015), J. Superlat. and Microstr. 65, 285–298.
6. Y. S. Kobayashi, H. Narita, T. Kanehira, K. Sonezaki, S. Kubota, Y. Terasaka, S. Iwasaki, (2010), Photochem. Photobiol., 86, 964 - 971.
7. Z. He, J. Liu, J. Miao, B. Liu, T. Thatt, (2014) J Mater Chem C (2), 1381-1385.
8. S. S. Mali, C. A. Betty, P.N. Bhosale, P.S. Patil (2011) J Cryst.Eng.Comm.13,6349-6351.
9. C.W. Kim, U. Pal, S. Park, Y.H. Kim, J. Kim, Y.S. Kang, (2012) RSC Adv. 2, 11969.
10. M. Salari, S. H. Aboutalebi, A. Aghassi, P. Wagner, A.J. Mozer, G.G. Wallace, (2015) Phys. Chem.17, 5642.
11. J. Li, W. Wan, H. Zhou, J. Li and, D. Xu, (2012) Chem. Commun., 48, 389-393.
12. D. B. Shinde, S. K. Jagadale, R. K. Mane, R. M. Mane, S.S. Mali, C. K. Hong and P. N. Bhosale, (2015), J. Nanomed. Nanotech. S7:004, 2157-7439.
13. P. S. Shinde, P. S. Patil, P. N. Bhosale, C. H. Bhosale, (2008), J. Appl. Catal. B: Env., 89, 288-293.
14. G. Poongodi, P. Anandan, R. M. Kumar, R. Jayavel, (2015), J. Pectrochimica Acta Part A. Mol. and Biomol. Spectro., 148, 237–243.
15. P. B. Patil, S. S. Mali, V.V. Kondalkar, N. B. Pawar, K. V. Khot, C. K. Hong, P. S. Patil, P. N. Bhosale, (2014), RSC Adv. 4, 47278.
16. D. B. Shinde, P. N. Bhosale and R. K. Mane (2018) J. AIIRJ, Vol.-V, III, 32-36.
17. S. Hoang, S. Guo, N. T. Hahn, A. J. Bard, C. B. Mullins, Nano Lett., (2011), 12, 26–32.
18. J. R. Jennings, A. Ghicov, L. M. Peter, P. Schmuki and A. B. Walker, J. Am. Chem. Soc., (2008), 130, 13364–13372.